VII Brazilian Symposium on Rock Mechanics – SBMR 2016
Rock Mechanics and Rock Engineering for Innovation and Development
ISRM Specialized Conference 19-22 October, Belo Horizonte, Minas Gerais, Brazil

A Review of the Models to Obtain Internal Friction Angle and Cohesion during Plastic Behavior for Weakly Consolidated Reservoirs – SBMR 2016

Juan Carlos Valenzuela Meza
Universidad Nacional de Colombia, Medellín, Colombia, jvalenzuelam@unal.edu.co

Edson Felipe Araujo Guerrero
Universidad Nacional de Colombia, Medellín, Colombia, efaraujog@unal.edu.co

Alejandra Arbelaez Londoño
Universidad Nacional de Colombia, Medellín, Colombia, aarbelal@unal.edu.co

Guillermo Alzate Espinosa
Universidad Nacional de Colombia, Medellín, Colombia, gaalzate@unal.edu.co

Abel Naranjo Agudelo
Universidad Nacional de Colombia, Medellín, Colombia, anaranjo@unal.edu.co

SUMMARY: Nowadays, heavy oil resources are the world's great petroleum deposits worldwide. These reservoirs are typically poorly or unconsolidated formations and characterized by having deforming permanently under the influence of mechanical stresses. During plastic strain, reservoir can exhibit irreversible changes that could generate sand production, well instability, subsidence, and changes in petrophysical properties such as porosity and permeability or mechanical properties such as elastic modules, tension strength, uniaxial compressive strength (UCS), among others. To prevent these harmful events and in order to make assertive predictions of their occurrence, it is necessary to study the effect of the change in the rock properties during plastic strain using coupled reservoir simulation. This paper presents a review of the basic existing models in the literature, which predict the behavior of the angle of internal friction and cohesion of the rock under a plastic strain regime. It presents that most models propose mathematical expressions to describe the behavior of the properties in function of plastic strain. Each model incorporates different parameters to quantify the level of plastic strain. However, these parameters do not correlate with variables of direct measurement and apply only to certain tests. As a result, this work performs a comparative analysis between the parameters and their behavior with the studied properties. In addition, it conducts a simulation of elastic and plastic regimes of rock behavior using a progressive algorithm under the basic assumptions of the plasticity theory and the failure criteria of Mohr-Coulomb with a yield surface of bilinear behavior. This algorithm solves stresses and strains for each increment of axial displacement for a Triaxial Compressive Strength Test. The results of the simulation show that the accumulator parameters of plastic strain exhibit a similar behavior respect to friction angle and cohesion but these parameters differ in magnitude. Additionally, the yield surface mobilization during the softening and hardening regimes is similar to the mobilization described in the literature. Finally, this work intends to develop subsequent analysis and to generate accurate relationships to model the behavior of the friction angle and cohesion in the plastic region.

KEYWORDS: Plastic regime, friction angle, cohesion, hardening, softening, yield surface.

1 INTRODUCTION

Changes of the friction angle, cohesion and dilation angle, which are parameters used in the Mohr-Coulomb failure criterion for modeling a yield surface rule the behavior of elastoplastic regime in sandstones. Understanding the mobilization of this surface is essential to simulate accurately the hardening/softening behavior experienced by the rock during plastic strain, which is essential for modeling the damage in the sandstones.

Mostly in literature, the modeling of friction angle, dilation angle and cohesion during hardening and softening behavior focuses on triaxial test simulation. This is one topic in the study of plastic behavior of rock and generally, the simulation of sand production and wellbore stability relates it. Papanastasiou and Vardoulakis (1992) conducted a study on the phenomenon of localization in relation to borehole stability, in which has been included a description of the behavior of the studied properties. Sulem et al. (1999) proposed that the plastic behavior of sandstones can be modeled using the friction hardening and cohesion softening under Mohr-Coulomb failure criterion. Later, Nouri et al. (2009) employs similar method to that proposed by Sulem's work to describe the elastoplastic behavior including a bilinear yield surface under the same failure criterion. Jafarpour et al. (2012) conducted some modifications to Sulem's work preserving the bilinear yield surface by Nouri, and accentuating the inclusion of an exponential function in the simulation of the softening behavior, which eliminates the assumption of uniform strain. Peng et al. (2013) proposed a softening behavior simulation based on the progressive failure of the rock, which is the continuation of work of Cai et al. (2007). Cai et al. (2007) postulates the use of Geological Strength Index (GSI) as a function of the plastic strain and a parameter mobilization of the yield surface in the Hoek-Brown failure criterion.

This paper reviews the most relevant models proposed by the authors presented above and finds that the behavior schematized for the studied properties depends on the equations used in each model and largely in the different parameters used as independent variables in these equations. Later, this performs an analysis between the studied properties and parameters. For this analysis, it has been implemented a progressive algorithm for simulation of the behavior of the rock in which the results of a triaxial test are taken as a baseline data.

2 MODELS

Focusing on the friction angle and cohesion changes, exist works that address the direct modeling of these properties and that additionally provide an experimental development. We choose some of them to evaluate its accuracy with data from a triaxial test for a poorly consolidated rock. In that sense, the works of Papanastasiou and Vardoulakis (1992), Nouri et al. (2009) and Jafarpour et al. (2012) are chosen. Peng's model (2013) is not included in this analysis because it does not include the change of the studied properties as an input for the mobilization of the yield surface.

The development of a continuous model and the poroelastic and poroelastic-plastic theories are the basis of selected models. This approaches are the most common used in geomechanics to describe the distribution of stresses and strains in sandstones. In addition, these models consider a combination of hardening and softening behaviors and employ a bilinear yield surface corresponding to the stress loading. These are classified in High Effective Confining Stress (HECS) and Low Effective Confining Stresses (LECS), for which a predominant regime hardening and softening is associated, respectively.

2.1 Model Parameters

For each of the models, the friction angle and cohesion simulation uses a mathematical parameter to describe the behavior of these properties. Nouri et al. (2009) uses the *plastic shear strain intensity* (g_p), Jafarpour et al. (2012) proposes the *hardening parameter rate* (h_p), and Papanastasiou and Vardoulakis (1992) establish the increment of *shearing-hardening parameter* (e^{ps}). These parameters consist of mathematical expressions, which have the function to cumulate both radial and axial plastic strains, and these are defined as,

$$\dot{g}_p = \sqrt{\frac{1}{2}\left(\dot{\varepsilon}^p_{ij} - \frac{1}{3}\dot{\varepsilon}^p_{kk}\delta_{ij}\right)\left(\dot{\varepsilon}^p_{ij} - \frac{1}{3}\dot{\varepsilon}^p_{kk}\delta_{ij}\right)} \quad (1)$$

Where δ_{ij} is the Kroneker tensor and the superscript p is refers to plastic strain.

$$\dot{h}_p = \frac{\sqrt{\left(\dot{e}^p_z\right)^2 + \left(\dot{e}^p_r\right)^2} - \dot{e}^p_z\dot{e}^p_r}{3} \quad (2)$$

$$\dot{e}^{ps} = \sqrt{\frac{1}{2}\left(\dot{e}^{ps}_1 - \dot{e}^{ps}_m\right)^2 + \frac{1}{2}\dot{e}^{ps\,2}_m + \frac{1}{2}\left(\dot{e}^{ps}_3 - \dot{e}^{ps}_m\right)^2} \quad (3)$$

Where,

$$\dot{e}^{ps}_m = \frac{1}{3}\left(\dot{e}^{ps}_1 + \dot{e}^{ps}_3\right) \quad (4)$$

2.2 Friction angle.

The three models consider that the friction angle increases parabolically during the hardening to a maximum value. After this, the friction angle remains constant in a value corresponding to the softening. The equations used to determine the behavior of the friction angle are:

2.2.1 Model of Jafarpour et al. (2012) and Nouri et al. (2009).

$$\varphi \begin{cases} \sin^{-1}\left(y_o + \frac{(m_1 - m_2 x_p)x_p}{1 + m_0 x_p}\right) & 0 \le x_p \le x^p_p \\ \varphi^p & x_p \ge x^p_p \end{cases} \quad (5)$$

Where x_p can be replaced by h_p or g_p. y_o is a value related to the initial angle friction, φ^p is the angle friction fully mobilized, m_0, m_1 and m_2 are parameters of material, and x^p_p can be replaced by h^p_p and g^p_p, respectively, corresponding to maximum stress reached.

2.2.2 Model of Papanastasiou-Vardoulakis (1992).

$$\sin\varphi^* = \begin{cases} 2\frac{\sqrt{e^{-ps}\varepsilon^f}}{e^{-ps} + \varepsilon^f}\sin\varphi & \text{for } e^{-ps} \le \varepsilon^f \\ & (1) \\ \sin\varphi & \text{for } e^{-ps} \ge \varepsilon^f \end{cases} \quad (6)$$

Where φ^* is the friction angle, φ is the friction angle fully mobilized, and ε^f is a value which determines if the angle friction has a constant behavior.

2.3 Cohesion

Cohesion behavior does not present a schematic behavior similar for the three models. For Papanastasiou-Vardoulakis (1992), cohesion has an initial value which declines immediately after plastic strain begins; this de-growth is presented as a reverse parabola with a turning point determined by a constant. In contrast to the other two work experiences, the cohesion increases during hardening, and subsequently it declines as reverse parabola during softening. However, the cohesion decline is different in each model. In the Jafarpour's work, the decline presents a turning point, which is nonexistent in Nouri's work. The equations used for modeling of cohesion for each work are below.

2.3.1 Model of Nouri et al. (2009).

$$q = \begin{cases} q_o & 0 \le g_p \le g^p_p \\ q_o - c_q\left(g_p - g^p_p\right)^2 & g_p \ge g^p_p \end{cases} \quad (7)$$

Where q_o is the tension cut-off, c_q is an adjustment parameter and g^p_p corresponds to the parameter value g_p in which hardening is changed to softening. The q value is related to cohesion through Equation (8),

$$c = -\tan\varphi * q \quad (8)$$

2.3.2 Model of Jafarpour et al. (2012) and Papanastasiou and Vardoulakis (1992).

$$c^* = c^p \exp\left[-\left(\frac{X}{Y_c}\right)^2\right] \quad (9)$$

Where X can be replaced by h_p - h_p^p for the work of Jafarpour and by e^{-ps} for the work of Papanastasiou and Vardoulakis, c^* is the cohesion, c^p is the reached cohesion for the maximum stress value, and Y_c is an adjustment parameter.

Equations (5), (6) and (9) help to model the properties of the rock for both HECS and LECS. Equations (7) and (8) help only to model for LECS state because its author considers that there is a change in q value for HECS state during hardening. However, this value is only the projection of a yield surface in HECS and it does not represent any real property of the rock and for this reason, it is not included in the work.

2.4 Dilation angle

For the dilation angle behavior, the three models use an equation proposed by Rowe (1972), in which the dilation angle changes as a function of angle of friction:

$$\sin\psi = \frac{\sin\varphi - \sin\varphi_{cv}}{1 - \sin\varphi \sin\varphi_{cv}} \tag{10}$$

Where φ_{cv} is the friction angle at constant volume, which can be calculated from dilation and friction angles at the maximum reached stress. The dilation angle behavior is similar to the friction angle, which has a parabolic growth during hardening and remains constant during softening.

3 MODELS COMPARISON

As mentioned earlier, the schematic behavior of the friction angle presented in the three works is similar: However, the model's equations have big differences in their mathematical description. In cohesion modeling, it shows similarities in schematic behavior between Nouri and Jafarpour models employing different equations. On the other hand, the schematic behavior is different for Jafarpour et al. (2012) model and Papanastasiou-Vardoulakis (1992) model using the same equation. These results are due to the parameters used in the models, which play a decisive role in the behavior of friction angle and cohesion.

For comparison of the behavior of each of these parameters with studied properties is essential to evaluate the three parameters in the same triaxial test. Therefore, it is performed a numerical simulation of a triaxial test with the purpose of obtaining the plastic strain, and therefore to calculate the parameters and their behavior.

4 SIMULATION ALGORITHM

The simulation algorithm uses the Mohr-coulomb failure criterion to simulate the elastoplastic region. It assumes that the total strain rate can divide into elastic and plastic parts, and that only the change of elastic strains influences the variation of stress through a constitutive law. For each time step of simulation, it calculates a new set of stresses based in an increase of the total strain through Hooke's law. If this new stresses are above the yield surface, a correction associated to plastic strain is applied to get the real new stress state.

The positive principal stress σ_1, σ_2, σ_3, correspond to compressive stress, and the initial value and variation of stress σ_2 and σ_3 are constants as it happens in a triaxial test. In order to use a system of dynamic explicit solution, it is considered to use linear elastic and plastic constitutive laws. The stress used are effective stress. The incremental expression of Hooke's law in terms of the effective stress and the strain has the following form:

$$\Delta\sigma_i = \alpha_1 \Delta e_i^e + \alpha_2 \left(\Delta e_j^e + \Delta e_k^e\right) \tag{11}$$

Where α_1 = K +4G/3 y α_2 =K-2G/3.

The yield function for shear in the Mohr-Coulomb failure criteria for the σ_1 vs σ_2 and σ_1 vs σ_3 planes are as follows,

$$\begin{aligned} f^1 &= \sigma_1 - \sigma_2 N\varphi - 2c\sqrt{N\varphi} \\ f^2 &= \sigma_1 - \sigma_3 N\varphi - 2c\sqrt{N\varphi} \end{aligned} \tag{12}$$

Where f is the function that determines the boundary condition of stresses in the plastic region, φ is the friction angle and c is cohesion and N_φ is equal to

$$N_{\varphi} = \frac{1+\sin\varphi}{1-\sin\varphi} \quad (13)$$

The plastic flow rule associated with the failure criterion Mohr-Coulomb corresponding $\sigma_1 = \sigma_2$ has the form of,

$$\Delta e_i^p = \lambda_1 \frac{\delta g^1}{\delta \sigma_i} + \lambda_2 \frac{\delta g^2}{\delta \sigma_i} \quad (14)$$

Where g^1 and g^2 are the corresponding potential functions to f^1 and f^2.

$$g^1 = \sigma_1 - \sigma_3 N_{\psi}$$
$$g^2 = \sigma_1 - \sigma_2 N_{\psi} \quad (15)$$

With ψ as the dilation angle and the parameter λ as follows,

$$N_{\psi} = \frac{1+\sin\psi}{1-\sin\psi} \quad (16)$$

$$\lambda = \frac{f^s(\sigma_1^I, \sigma_3^I)}{(\alpha_1 - \alpha_2 N_{\psi}) - (\alpha_2 - \alpha_1 N_{\psi}) N_{\varphi}} \quad (17)$$

Where f^s is the yield function and σ_1^I, σ_3^I are the calculated stress assuming that all total strain increments causes changes in the stress.

5 RESULTS

The simulation of the behavior of the rock in the elastic and plastic region for a high confinement stresses HECS state is performed. The basic experimental data used correspond to the results of a triaxial test at 17.23 MPa confinement pressure for an unconsolidated formation, Castlegate field, reported in Jafarpour et al. (2012). As an input data to generate the rock plastic behavior and yield surface is necessary to know the properties of the rock in the elastic region, which are the starting point of the plastic region. The elastic properties are calculated at 50% of the stress peak as recommended by Schanz et al. (1999). The Young modulus and Poisson's ratio are calculated by:

$$E = \frac{\sigma_z}{\varepsilon_z} \quad (18)$$

$$\nu = -\frac{\varepsilon_r}{\varepsilon_z} \quad (19)$$

The data for the initial friction angle, initial dilation angle and initial cohesion are found in the Jafarpour's work, and its values are shown at Table 1.

Table 1. Elastic properties

Data	
Young modulus, MPa	5562,7
Poisson's ratio	0,085
Initial dilation angle. °	10
Initial friction angle, °	18,518
Initial Cohesion, MPa	6
Tensile strength, MPa	7,58

The simulation is performed with a Δt of 2 min and a strain rate of 0.001 cm/min. It reaches a corresponding axial strain 9.7% in 2500 steps. The simulation results and the digitized data are in Figure 1.

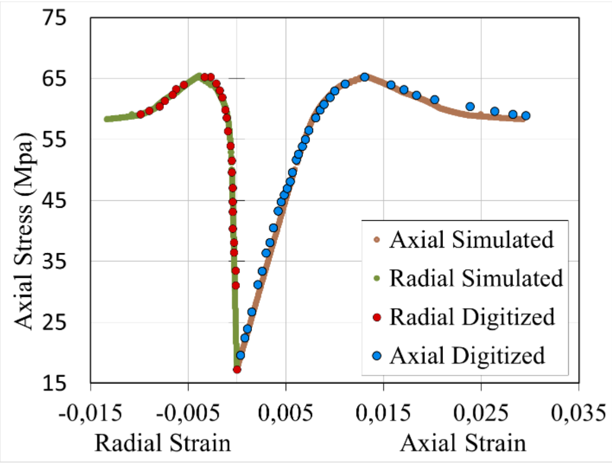

Figure 1. Simulation and digitized results of triaxial test used to compare the data behavior and selected models.

As shown in Figure 1, the simulation results reproduce satisfactorily the behavior of the experimental data, as result of the properly selection of the elastic modulus. This simulation does not include the localization phenomenon presented in softening. The similar behavior is the result of the right choice of changing the friction angle and cohesion.

5.1 Yield Surface

The mobilization of the yield surface in the simulation of the rock under Mohr-Coulomb failure criteria is shown in Figure 2.

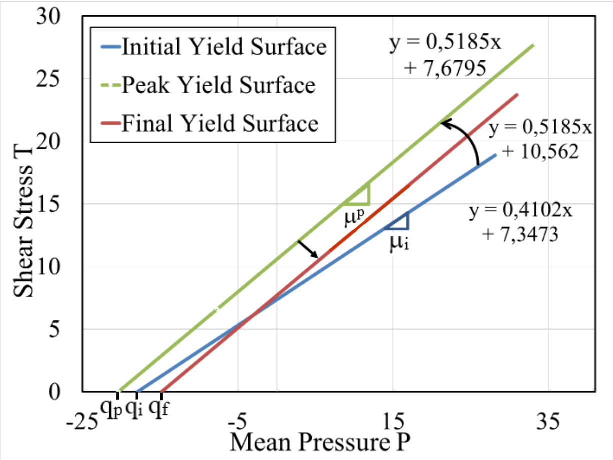

Figure 2. Motion of the yield surface in the T-P stress space.

The surface is provided in the plane T-P, where T is the square root of the second invariant of the deviatoric stress tensor, and P is the mean effective stress. For the simulated triaxial test, P and T corresponds to:

$$P = -\left(\sigma'_z + 2\sigma'_r\right)/3 \qquad (20)$$
$$T = \left|\sigma'_z - 2\sigma'_r\right| / \sqrt{3}$$

The yield surface that works on the algorithm for the plane T-P is described by:

$$F = T - (q + P)\,\mu = 0 \qquad (21)$$

Where $\mu = \tan \varphi_\sigma$ and $\tan \varphi_\sigma$ is the friction coefficient can be related to the angle of friction (φ) through Equation (22),

$$\tan \varphi_\sigma = \frac{2\sqrt{3}\sin\varphi}{3 - \sin\varphi} \qquad (22)$$

And q is the tension, which can be related to the cohesion, c, as:

$$q = -\frac{c}{\tan \varphi} \qquad (23)$$

The yield surface obtained from the simulation presents an expansion of the yield surface during hardening and contraction during softening, which is in line with the guidelines set in the studied models.

Because the performed simulation only considers the behavior of the rock in HECS, only one is presented in Figure 2, where part of this line correspond to LECS and does not represent the true yield surface because this part is a projection of behavior in HECS. The motion of yield surface presented in Figure 2 begins when a stress state reaches the initial surface and the plastic strain appears. After that, the initial surface friction coefficient (μ_i) with a value of 0.4102 increases until the yield surface is mobilized to the peak surface (μ^p) taking a value of 0.518.

In the studied models, bilinear surface is assumed that intercepts with the p axis for initial and peak surface is constant in the LECS state, which implies that no microcracks are generated during this step. However, for the HECS state has not consensus on whether this value is constant or varies. In the simulation, the intersection point varies in 2.4 MPa, approximating the behavior of this surface to the proposal made in the Nouri’s work. These mobilization yield surfaces represent the hardening of the rock. Following this, the yield surface moves from peak surface to end surface. This step corresponds to softening of the rock. The value of the coefficient of friction during this stage remains constant throughout the process at a value of 0.518. The yield surface shrinkage is attributed to the decrease in tensile strength (q), which is reflected in the appearance of microfractures in the rock. This value decays to zero when the rock loses its cohesion and is completely disaggregated.

With the behavior of the yield surface, the friction angle presents a schematic mobilization according to the three reviewed models, in which the angle varies during hardening and remains constant during softening. On the other hand, because during HECS, the intersection of the yield surface with the p axis (q) is only a line projection and does not related to rock properties, then Equation (22) cannot be used to find the value of the real cohesion.

5.2 Properties and parameters

As mentioned above, the friction angle behavior is consistent with the proposed models studied. In the simulation during hardening, the friction angle changes from 18.51 to 22.9 in a polynomial form. Subsequently, during softening, its value maintains about 22.9. The behavior of friction angle and the different accumulators' parameters are shown in Figure 3.

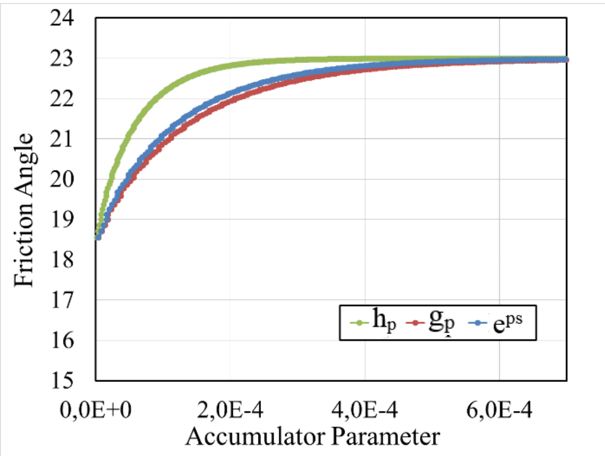

Figure 3. Behavior of friction angle against the accumulators' parameters.

As shown in Figure 3, the friction angle behavior as a function of g_p, h_p and e^{ps} is similar and just changes in the magnitude value depending on each parameter. Additionally, it is found that the corresponding functions g_p and e^{ps} are practically superimposed even though the mathematical calculation is different.

The behavior of the cohesion during plastic strain increases from an initial cohesion 6 MPa to 8.64 MPa, corresponding to the hardening step. After this, the value decays to 6.3 MPa during softening. The behavior of the cohesion in function of the accumulative parameters g_p, h_p and e^{ps} is presented in Figure 4.

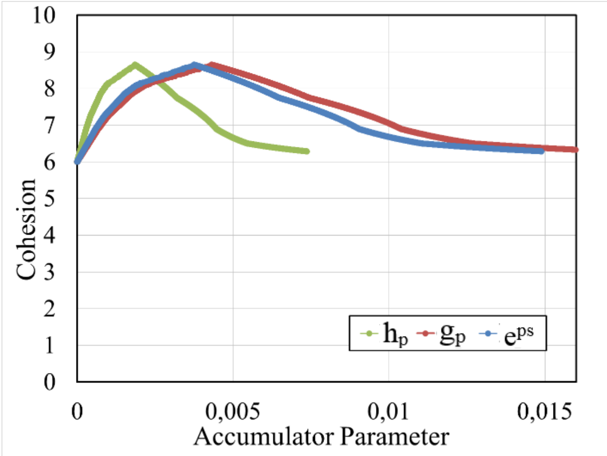

Figure 4. Behavior of cohesion as a function the accumulator's parameters.

As shown in Figure 4, cohesion behavior for different parameters is similar in shape but different in magnitude. It is important to note that the initial growth of cohesion is not consistent with the model presented in Papanastasiou-Vardoulakis, which assumes an increase in cohesion. This is because of it considers the magnitude of this increment is negligible.

Finally, although the parameters g_p, h_p and e^{ps} have been proposed for specific tests and have different mathematical expressions in relation to plastic strain, Figures 3 and 4 show that its relationship with the behavior of the studied properties are the same. This can be attributed to the relationship found between increased parameters and plastic strain, for which in the three cases exhibit a linear behavior.

5 CONCLUSIONS

Reviewing the models leads to conclude that parameters exhibit a key role in modeling the properties. In addition, regardless of the variation of the mathematical expression of each accumulator parameter, these have the plastic strains as fundamental input.

The simulation performed using the proposed algorithm under Mohr-Coulomb failure criterion and considering a bilinear yield surface is able to reproduce accurately the behavior of the rock. However, the appropriate choice of elastic properties is essential.

The mobilization of yield surface is a result of changing the friction angle and cohesion to adjust the real behavior of the rock. Then, the mobilization is consistent with the one found in the studied models.

The behavior of the studied properties within the simulation is similar to that obtained for experimental data, achieving a high degree of assertiveness of the results obtained.

For comparison, the accumulator parameters are effective tools for the understanding of the evaluated properties. It is evidenced that regardless of the selected parameter for the same triaxial test, cohesion and friction presented a similar behavior with variation only in magnitude.

REFERENCES

Cai, M., Kaiser, P. K. and Tasaka, Y. (2007). Determination of residual strength parameters of jointed rock masses using the GSI system. *International Journal of Rock Mechanics and Mining Sciences*, vol. 44 (2), p. 247-265.

Jafarpour, M., Rahmati, H., Azadbakht, S., Nouri, A., Chan, D. and Vaziri, H. (2012). Determination of mobilized strength properties of degrading sandstone. *Soils and Foundations*, vol. *52*, p. 658–667. http://doi.org/10.1016/j.sandf.2012.07.007.

Nouri, A., Kuru, E., and Vaziri, H. (2009). Elastoplastic Modelling of Sand Production Using Fracture Energy Regularization Method. *Journal of Canadian Petroleum Technology*, vol 48 (4), p. 64–71. http://doi.org/10.2118/09-04-64.

Papanastasiou, P. and Vardoulakis, I. (1992). Numerical Treatment of Progressive Localization in Relation to Borehole Stability. *Journal Numer Analyt Methods Geomech*, vol 16 (6), p. 389–424.

Peng, J., Rong, G., Zhou, C., Cai, M., and Du, W. (2013). Simulating Brittle Failure of Rocks by a new Strain-Softening Model. *47th US Rock Mechanics/Geomechanics Symposium, 23-26 june, San Francisco*, vol 3, p. 2112-2118

Rowe, P. W. (1972). Theoretical Meaning and Observed Values of Deformation Parameters for Soils. *In:Proceeding of the Roscoe Memorial Symposium on Stress-Strain Behaviour of Soils, Cambridge, Foulis, Henley-on-Thames*, p. 143-194.

Schanz, T., Vermeer, P. A., and Bonnier, P. G. (1999). The Hardening Soil Model: Formulation and Verification. *In: proceedings Plaxis Symposium beyond 2000 in computational geotechnics, Amsterdam, Balkema*, p. 281-296.

Sulem, J., Vardoulakis, I., Papamichos, E. Oulahna, A., and Tronvoll, J. (1999). Elastoplastic Modeling of Red Wildmoor Sandstone. *Mechanics of Cohesive-Frictional Materials*, vol. *4*, p. 215–245.